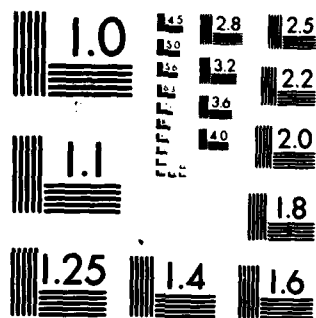


AD-A087 429

UNCLASSIFIED

OKLAHOMA UNIV NORMAN SCHOOL OF AEROSPACE MECHANICAL --ETC F/S 11/4
THERMOELASTICITY OF CIRCULAR CYLINDRICAL SHELLS LAMINATED OF BI--ETC(U)
JUL 80 Y S HSU, J N REDDY, C W BERT N00014-T8-C-0647
OU-AMNE-80-14 NL

END
DATE
FILMED
9 80
DTIC



MICROCOPY RESOLUTION TEST CHART
NATIONAL BUREAU OF STANDARDS 1963-A

ADA 087429

154
LEVEL # 12
Department of the Navy
OFFICE OF NAVAL RESEARCH
Structural Mechanics Program
Arlington, Virginia 22217

15 Contract N00014-78-C-0647
Project NR 064-609

9 Technical Report No. 17

14 Report CU-AMNE-80-14, TR-17

6 THERMOELASTICITY OF CIRCULAR CYLINDRICAL SHELLS
LAMINATED OF BIMODULUS COMPOSITE MATERIALS.

by

10 Y.S./Hsu, J.N./Reddy, C.W./Bert

11 Jul 1980

12 38
DTIC
ELECTE
AUG 4 1980
S A

School of Aerospace, Mechanical and Nuclear Engineering
University of Oklahoma
Norman, Oklahoma 73019

Approved for public release; distribution unlimited

DOC FILE COPY

80

8

1

014

100498

THERMOELASTICITY OF CIRCULAR CYLINDRICAL SHELLS LAMINATED OF BIMODULUS COMPOSITE MATERIALS

Y.S. Hsu, J.N. Reddy, and C.W. Bert
School of Aerospace, Mechanical and Nuclear Engineering
University of Oklahoma, Norman, OK 73019

✓
Closed-form and finite-element solutions are presented for the thermoelastic behavior of laminated composite shells. The material of each layer is assumed to be thermoelastically orthotropic and bimodular, i.e., having different properties depending upon whether the fiber-direction normal strain is tensile or compressive. The formulations are based on the thermoelastic generalization of Dong and Tso's laminated shell theory, which includes thickness shear deformations. The finite element used here has five degrees of freedom per node (three displacements and two bending slopes). Numerical results are presented for deflections and the positions of the neutral surfaces associated with bending along both coordinate directions. The closed-form and finite-element results are found to be in good agreement.

INTRODUCTION

As the field of composite-material mechanics becomes more highly developed, increasing attention is being given to the development of more realistic models of actual material behavior and to the application of these models to thermostructural analysis of composite-material structural elements such as plates and shells. Certain fiber-reinforced composite materials, especially

Availability Codes	
Dist	Avail and/or special
A	

those with very soft matrices, exhibit the interesting phenomenon of having quite different elastic properties when loaded along the fiber direction in tension as contrasted to compression. This was demonstrated for cord-rubber composites by Clark [1] and Patel et al. [2]. The first attempt to formulate a theory of elastic behavior of such materials was due to Ambartsumyan [3], and a comprehensive theory consistent with experimental results was introduced in [4] and further discussed in [5].

Most of the thermoelastic analyses of bimodulus-material structural elements [6-12] have been limited to isotropic bimodulus materials. However, in a recently developed theory of micromechanics of fiber-reinforced materials with soft matrices [13], it was shown that the thermal-expansion coefficients, as well as the elastic properties, should depend upon the sign of the fiber-direction strain. Unfortunately, there does not appear to be any appropriate experimental data available to date to confirm this conclusion and to provide quantitative values for the thermal-expansion coefficients. To the best of the knowledge of the current investigators, the only analysis to provide for the bimodular effect on thermal expansion is a very recent thermoelastic analysis of thick laminated plates [14].

There have been a few thermoelastic analyses of shells laminated of ordinary composite materials. Stavsky and Smolash [15] considered thin, laminated, orthotropic shells using Love's first-approximation shell theory, and Pao [16] treated similar shells using Flügge's higher-order thin-shell theory. Recently, Padovan and Lestingi [17] analyzed heated anisotropic shells including thickness-shear deformation.

A number of analyses of various kinds of bimodulus shells have appeared in the literature; ten of them were reviewed in [18]. However, in every

instance they treated only thin shells subjected to mechanical loading only.

The present analysis is believed to be the first analysis of bimodulus shells to include either thermal loading or thickness-shear deformation. The theory used is a generalized first-approximation thermoelastic shell theory which can be reduced by means of tracer coefficients to various simpler theories.

GOVERNING EQUATIONS

Let x and y denote the axial and circumferential position coordinates measured on the shell middle surface, and z the outward normal position coordinate (see Figure 1).

The displacement field at an arbitrary location (x,y,z) is given by

$$\begin{aligned} U(x,y,z) &= u(x,y) + z\beta_x(x,y) \\ V(x,y,z) &= v(x,y) + z\beta_y(x,y) \\ W(x,y,z) &= w(x,y) \end{aligned} \quad (1)$$

Here, u,v,w are the middle-surface displacements, and β_x and β_y are the bending slopes.

The strain-displacement relations for small deflections can be written as

$$\epsilon_i = \epsilon_i^0 + z\kappa_i \quad (i=1,2,4,5,6) \quad (2)$$

Here, ϵ_i are the engineering-strain components at an arbitrary location (x,y,z) , ϵ_j^0 are the engineering-strain components on the middle surface $(x,y,0)$, and κ_i are the curvature changes. The notation of classical composite-material mechanics is used, with 1 and 2 denoting normal action in

directions x and y , respectively, and 6 denoting shear action with respect to x, y axes. Now

$$\begin{aligned}
 \epsilon_1^0 &= u_{,x} \quad , \quad \epsilon_2^0 = v_{,y} + (w/R) \quad , \quad \epsilon_6^0 = u_{,y} + v_{,x} \\
 \epsilon_4^0 &= \beta_y + w_{,y} - (C_1/R)v \quad , \quad \epsilon_5^0 = \beta_x + w_{,x} \\
 \kappa_1 &= \beta_{x,x} \quad , \quad \kappa_2 = \beta_{y,y} \quad , \quad \kappa_6 = \beta_{x,y} + \beta_{y,x} \\
 &\quad \quad \quad \quad \quad \quad \quad \quad + (C_2/2R)(v_{,x} - u_{,y}) \\
 \kappa_4 &= \kappa_5 = 0
 \end{aligned} \tag{3}$$

Here, R is the radius of the middle-surface, the C_i are shell-theory tracers to be discussed later, and $(\quad)_{,x} \equiv \partial(\quad)/\partial x$.

Considering the shell to consist of either a single orthotropic layer or to be a cross-ply laminate (one having all layers oriented at either 0° or 90° with respect to the cylinder axis), the thermoelastic version of generalized Hooke's law may be written as follows for each layer:

$$\begin{Bmatrix} \sigma_1 \\ \sigma_2 \\ \sigma_4 \\ \sigma_5 \\ \sigma_6 \end{Bmatrix} = \begin{bmatrix} Q_{11kl} & Q_{12kl} & 0 & 0 & 0 \\ Q_{12kl} & Q_{22kl} & 0 & 0 & 0 \\ 0 & 0 & Q_{44kl} & 0 & 0 \\ 0 & 0 & 0 & Q_{55kl} & 0 \\ 0 & 0 & 0 & 0 & Q_{66kl} \end{bmatrix} \begin{Bmatrix} \epsilon_1 - \alpha_{1kl}T \\ \epsilon_2 - \alpha_{2kl}T \\ \epsilon_4 \\ \epsilon_5 \\ \epsilon_6 \end{Bmatrix} \tag{4}$$

Here, σ_i are the stress components, Q_{ijkl} are the plane-stress-reduced stiffnesses, α_{jkl} are the thermal expansion coefficients, and T is the temperature measured from the strain-free temperature. Subscript $k=1$ for fiber-direction tension and 2 for compression, and subscript ℓ denotes the layer number.

The stress resultants and stress couples are defined in the customary

way for a first-approximation shell theory as

$$(N_i, M_i) = \int_{-h/2}^{h/2} (1, z) \sigma_i dz \quad (5)$$

where $h \equiv$ total laminate thickness. Similarly, thermoelastic stress resultants and stress couples are defined as

$$(N_i^T, M_i^T) = \int_{-h/2}^{h/2} (1, z) E_{ikl} dz \quad (6)$$

where

$$E_{ikl} = Q_{ijkl} \alpha_{jkl} \quad (\text{no sum on } k\ell) \quad (7)$$

Since thickness-shear deformation is included, the shear stress resultants are introduced

$$(Q_2, Q_1) = \int_{-h/2}^{h/2} (\sigma_4, \sigma_5) dz \quad (8)$$

Substituting Equations (4) and (6) into Equations (5) and (8), one obtains the following shell constitutive relations

$$\begin{Bmatrix} N_1 + N_1^T \\ N_2 + N_2^T \\ N_6 \\ Q_2 \\ Q_1 \\ M_1 + M_1^T \\ M_2 + M_2^T \\ M_6 \end{Bmatrix} = \begin{bmatrix} A_{11} & A_{12} & 0 & 0 & 0 & B_{11} & B_{12} & 0 \\ A_{12} & A_{22} & 0 & 0 & 0 & B_{12} & B_{22} & 0 \\ 0 & 0 & A_{66} & 0 & 0 & 0 & 0 & B_{66} \\ 0 & 0 & 0 & S_{44} & 0 & 0 & 0 & 0 \\ 0 & 0 & 0 & 0 & S_{55} & 0 & 0 & 0 \\ B_{11} & B_{12} & 0 & 0 & 0 & D_{11} & D_{12} & 0 \\ B_{12} & B_{22} & 0 & 0 & 0 & D_{12} & D_{22} & 0 \\ 0 & 0 & B_{66} & 0 & 0 & 0 & 0 & D_{66} \end{bmatrix} \begin{Bmatrix} \epsilon_1^0 \\ \epsilon_2^0 \\ \epsilon_6^0 \\ \epsilon_4 \\ \epsilon_5 \\ \kappa_1 \\ \kappa_2 \\ \kappa_6 \end{Bmatrix} \quad (9)$$

Here, A_{ij} = inplane stiffness, B_{ij} = inplane-bending coupling stiffness, D_{ij} = bending stiffness, S_{ij} = thickness shear stiffness, defined by

$$(A_{ij}, B_{ij}, D_{ij}) = \int_{-h/2}^{h/2} (1, z, z^2) Q_{ij} dz \quad (i, j=1, 2, 6) \quad (10)$$

$$S_{ij} = K^2 \int_{-h/2}^{h/2} Q_{ij} dz \quad (i, j=4, 5)$$

(Derivations of A_{ij} , B_{ij} , D_{ij} , N_i^T , and M_i^T are carried out in detail for a laminated bimodulus shell in Appendix A.)

The shell equilibrium equations, in the absence of body forces and body moments, can be written as

$$\begin{aligned} N_{1,x} + N_{6,y} - (C_2/2R)M_{6,y} &= 0 \\ N_{6,x} + N_{2,y} + (C_1/R)Q_2 + (C_2/2R)M_{6,x} &= 0 \\ Q_{1,x} + Q_{2,y} - (N_2/R) &= P \\ M_{1,x} + M_{6,y} &= Q_1 \quad ; \quad M_{6,x} + M_{2,y} = Q_2 \end{aligned} \quad (11)$$

where P is the normal pressure.

If the shell-theory tracer C_1 is set equal to unity and C_2 set equal to zero, the theory presented here can be considered to be the thermoelastic version of the shear-deformation shell theory of laminated, orthotropic, circular cylindrical shells presented by Dong and Tso [19]. This theory is the shear-deformable, laminated, orthotropic version of the well-known Love first-approximation shell theory [20], as modified by Reissner [21]; see also chap. 2 of [22].

If the shell-theory tracers are set equal to other values as specified in Table 1, the theory represents the shear-deformable, laminated orthotropic version of the Sanders "best" first-approximation theory [23], Loo's approximate theory [24], Morley's shallow-shell theory [25], and Donnell's very-shallow-shell theory [26]. It is interesting to note that when generalized to include shear deformation, one cannot distinguish between Love's first-approximation theory and Loo's theory and also between Morley's and Donnell's shallow-shell theories.

Substituting Equations (3) and (9) into Equations (11), we obtain the following operator equation

$$[L]\{\delta\} = \{f\} \quad (12)$$

where

$$\{\delta\} = \{u, v, w, \beta_x, \beta_y\}^T$$

Now $[L]$ is the symmetric matrix of the following differential operators:

$$\begin{aligned} L_{11} &= A_{11}d_x^2 + (A_{66} - \bar{C}_2B_{66} + \frac{1}{4}\bar{C}_2^2D_{66})d_y^2 \\ L_{12} &= (A_{12} + A_{66} - \frac{1}{4}\bar{C}_2^2D_{66})d_xd_y \\ L_{13} &= (A_{12}/R)d_x \quad ; \quad L_{14} = B_{11}d_x^2 + (B_{66} - \frac{1}{2}\bar{C}_2D_{66})d_y^2 \\ L_{15} &= (B_{12} + B_{66} - \frac{1}{2}\bar{C}_2D_{66})d_xd_y \\ L_{22} &= (A_{66} + \bar{C}_2B_{66} + \frac{1}{4}\bar{C}_2^2D_{66})d_x^2 + A_{22}d_y^2 - \bar{C}_1^2S_{44} \\ L_{23} &= (R^{-1}A_{22} + \bar{C}_1S_{44})d_y \quad ; \quad L_{24} = (B_{12} + B_{66} + \frac{1}{2}\bar{C}_2D_{66})d_xd_y \\ L_{25} &= (B_{66} + \frac{1}{2}\bar{C}_2D_{66})d_x^2 + B_{22}d_y^2 + \bar{C}_1S_{44} \\ L_{33} &= -S_{55}d_x^2 - S_{44}d_y^2 + (A_{22}/R^2) \\ L_{34} &= (R^{-1}B_{12} - S_{55})d_x \quad ; \quad L_{35} = (R^{-1}B_{22} - S_{44})d_y \end{aligned} \quad (13)$$

$$L_{44} = D_{11}d_x^2 + D_{66}d_y^2 - S_{55} \quad ; \quad L_{45} = (D_{12} + D_{66})d_x d_y$$

$$L_{55} = D_{66}d_x^2 + D_{22}d_y^2 - S_{44} \quad ; \quad \bar{C}_1 = C_1/R \quad ; \quad d_x = \partial(\quad)/\partial x, \text{ etc.}$$

Also the components of the generalized thermal-force vector $\{f\}$ are:

$$f_1 = N_{1,x}^T \quad ; \quad f_2 = N_{2,y}^T \quad ; \quad f_3 = P - (N_2^T/R)$$

$$f_4 = M_{1,x}^T \quad ; \quad f_5 = M_{2,y}^T \quad (14)$$

In view of the assumed linearity of the displacements with z , it is consistent to assume that the temperature distribution is also linear with z :

$$T(x,y,z) = T_0(x,y) + zT_1(x,y) \quad (15)$$

CRITERIA FOR HOMOGENEITY ALONG MIDDLE SURFACE

In deriving Equations (12), we tacitly assumed that the laminate stiffnesses $(A_{ij}, B_{ij}, D_{ij}, S_{ij})$ are all independent of coordinates (x,y) on the middle surface. However, in view of the bimodulus nature of the materials comprising the laminate, these stiffnesses depend upon the fiber-direction neutral-surface positions associated with the respective layers (i.e., z_{nx} for a single layer with axially oriented fibers, and z_{nx} and z_{ny} for a cross-ply laminate).

Thus, for layers having the fibers oriented axially, the associated fiber-direction neutral-surface position is determined by

$$\epsilon_1 = \epsilon_1^0 + z_{nx}\kappa_1 = 0$$

or

$$z_{nx} = -\epsilon_1^0/\kappa_1 = -u_{,x}/\beta_{x,x} = \text{constant} \quad (16)$$

Similarly, for layers having the fibers oriented circumferentially

$$\epsilon_2 = \epsilon_2^0 + z_{ny}\kappa_2 = 0$$

or

$$z_{ny} = -\epsilon_2^0/\kappa_2 - (v_{,y} + R^{-1}w)/\beta_{y,y} = \text{constant} \quad (17)$$

CLOSED-FORM SOLUTION

A solution is sought which satisfies the governing operator equation, Equation (12), the subsidiary relations, Equations (16) and (17), and the appropriate boundary conditions.

A closed-form solution has been found for the following conditions:

Loading (sinusoidally distributed):

$$\begin{aligned} P &= P_0 \sin \alpha x \sin \beta y, \quad T_0 = \bar{T}_0 \sin \alpha x \sin \beta y \\ T_1 &= \bar{T}_1 \sin \alpha x \sin \beta y, \quad \alpha = \pi x/a, \quad \beta = \pi y/b \end{aligned} \quad (18)$$

Here a and b are the dimensions of the shell in the respective axial and circumferential directions (see Fig. 1).

Boundary Conditions (freely supported):

$$\begin{aligned} N_1(0,y) &= N_1(a,y) = M_1(0,y) = M_1(a,y) = 0 \\ w(0,y) &= w(a,y) = v(0,y) = v(a,y) = 0 \\ N_2(x,0) &= N_2(x,b) = M_2(x,0) = M_2(x,b) = 0 \\ w(x,0) &= w(x,b) = u(x,0) = u(x,b) = 0 \\ \beta_y(0,y) &= \beta_y(a,y) = \beta_x(x,0) = \beta_x(x,b) = 0 \end{aligned} \quad (19)$$

Under these conditions, the solution to Equation (12) is of the form

$$\begin{aligned} u(x,y) &= \bar{U} \cos \alpha x \sin \beta y \\ v(x,y) &= \bar{V} \sin \alpha x \cos \beta y \\ w(x,y) &= \bar{W} \sin \alpha x \sin \beta y \\ \beta_x(x,y) &= \bar{X} \cos \alpha x \sin \beta y \\ \beta_y(x,y) &= \bar{Y} \sin \alpha x \cos \beta y \end{aligned} \quad (20)$$

Substitution of Equations (20) into Equation (12) leads to the following nonhomogeneous algebraic system:

$$[C]\{\Delta\} = \{F\} \quad (21)$$

where

$$\begin{aligned} \{\Delta\} &= \{\bar{U}, \bar{V}, \bar{W}, \bar{X}, \bar{Y}\}^T \\ \{F\} &= \{F_1, F_2, F_3, F_4, F_5\}^T \end{aligned} \quad (22)$$

The quantities F_r and the coefficients C_{rs} of the matrix $[C]$ are not presented here, for brevity.

For a given set α , β , P_0 , R , F_i and either single-layer or cross-ply construction, one needs to solve the 5x5 matrix Equation (21) for the vector $\{\Delta\}$ of amplitudes of the generalized displacements, subject to subsidiary conditions (16) and (17). For bimodulus-material shells, the laminate stiffnesses (A_{ij}, B_{ij}, D_{ij}) are, in general, not constant, but depend upon x and y through the fiber-direction neutral-surface positions (z_{nx} and z_{ny}). However, for the present combination of loading and boundary conditions, z_{nx} and z_{ny} are both constants, i.e., independent of x and y . Although it is conceptually possible to substitute the solution functions into Equations (16) and (17) to obtain cubic equations involving z_{nx} and z_{ny} , it is computationally much more efficient to satisfy Equations (16) and (17) by iterating on z_{nx} and z_{ny} .

FINITE-ELEMENT FORMULATION

Since an exact closed-form solution to Equation (12) can be obtained only under special conditions of geometry, edge conditions, loadings, and lamination, it is desirable to have available a more general method. Here, we develop a simple, mixed-type, finite-element formulation which has no

such limitations, except for those implied in the formulation of shear-flexible laminated shell theory.

Let the region R be subdivided into a finite number N of subregions: finite elements, R_e ($e=1,2,\dots,N$). Over each element, the generalized displacements (u,v,w,β_x,β_y) are interpolated according to

$$\begin{aligned} u &= \sum_i^r u_i \phi_i^1, & v &= \sum_i^r v_i \phi_i^1, & w &= \sum_i^s w_i \phi_i^2 \\ \beta_x &= \sum_i^p X_i \phi_i^3, & \beta_y &= \sum_i^p Y_i \phi_i^3 \end{aligned} \quad (23)$$

Here, ϕ_i^α ($\alpha=1,2,3$) is the interpolation function corresponding to the i -th node in the element. It is noted that the inplane displacements, the normal deflection, and the bending slopes may be approximated by different sets of interpolation functions. Although this generality is considered in the formulation presented here, when the element is actually programmed, we set $\phi^1 = \phi^2 = \phi^3$ ($r=s=p$) for simplicity. Noting that r , s , and p denote the number of degrees of freedom (DOF) for each variable, the total number of DOF per element is $2r + s + 2p$.

Substituting interpolations of the form (23) for u , v , w , β_x , and β_y into the Galerkin integrals associated with the governing operator equation (12), we obtain

$$\int_{R_e} ([L]\{\delta\} - \{f\})\{\phi\} dx dy = 0 \quad (24)$$

Now using integration by parts once in order to distribute the differentiation equally among the terms in each expression, we obtain the element equation

$$[K]_e \{\nabla\}_e = \{F\}_e \quad (25)$$

The elements $K_{ij}^{\alpha\beta}$ ($\alpha, \beta=1,2,\dots,5$) of the element stiffness matrix and \bar{F}_i^α of the generalized force vector are listed in Appendix B.

In the present investigation, cylindrically curved rectangular elements of the serendipity family are used, with the same interpolation for all of the variables. The resulting stiffness matrices are 20 by 20 for the four-node element and 40 by 40 for the eight-node element. Reduced integration [27,28] must be used to evaluate the matrix coefficients in Appendix B. For example, for the four-node rectangular element, the 1x1 Gauss rule must be used rather than the standard 2x2 Gauss rule.

NUMERICAL RESULTS

It would be desirable to compare the results obtained by the present analyses with those given in the literature for special cases. Unfortunately, however, there is a dearth of solutions of cylindrical panels subjected to sinusoidally distributed mechanical and thermal loadings. However, in a recent closed-form and finite-element study [14] of thermally loaded plates, good agreement was obtained with results presented by Boley and Weiner [29] for isotropic, thin plates.

As practical examples of orthotropic bimodulus materials, the same two unidirectional cord-rubber materials as considered in [14,18] are considered, namely, aramid-rubber and polyester-rubber. The inplane elastic properties were obtained from experimental results of [2] using the data-reduction procedure presented in [4]. Since the thickness-shear moduli were not measured in [2], they were estimated as described in detail in [30]. The elastic properties are listed in Table 2.

Unfortunately, the present investigators are unaware of any experimentally

determined values for the thermal-expansion coefficients of cord-rubber materials. However, the micromechanics analysis of bimodular action presented in [13] suggested that the thermal-expansion coefficients (α_1 and α_2) of these materials should also depend upon the sign of the fiber-direction strain. Thus, in the numerical calculations presented here, the following dimensionless relationships are used:

$$\alpha_1^t/\alpha_1^c = 0.5 \quad ; \quad \alpha_2^t/\alpha_2^c = 1.0 \quad ; \quad \alpha_1^t/\alpha_2^t = 0.1$$

Here, superscripts c and t refer to compressive and tensile fiber-direction strains.

Table 3 shows the effect of the radius-to-thickness ratio (R/h) on the locations of neutral surfaces and dimensionless deflections for single-layer and two-layer cross-ply aramid-rubber cylindrical panels under sinusoidal mechanical loading by Sanders theory. As the radius-to-thickness ratio is increased to infinity, the panel can be considered as a plate. Table 3 also shows the convergence of the dimensionless deflections.

Numerical results of the influence of the aspect ratio on the dimensionless deflections and neutral-surface locations for single-layer and two-layer cross-ply, freely supported cylindrical shells constructed of bimodulus materials and subjected to sinusoidal thermal loading ($R/h = 10$) by Sanders theory are shown in Tables 4 and 5, respectively. Again, there is a close agreement between the finite-element and closed-form results.

Figure 2 shows the effect of radius-to-thickness ratio and aspect ratio (a/b) on the dimensionless deflections and neutral-surface locations for one-layer and two-layer cross-ply, freely supported aramid-rubber cylindrical shells under sinusoidal thermal loading by Sanders theory.

Figures 3 and 4 show the influence of aspect ratio and radius-to-thickness ratio, respectively, on the locations of neutral surfaces for single-layer, freely supported, aramid-rubber cylindrical shells under sinusoidal thermal loading by Sanders theory. Similar results are shown in Figures 5 and 6 for two-layer cross-ply, freely-supported polyester-rubber cylindrical shells under sinusoidal thermal loading. As can be seen, there is only a slight change of neutral-surface locations for radius-to-thickness ratios greater than 60.

CONCLUDING REMARKS

A finite-element formulation of equations governing layered anisotropic composite shells subjected to mechanical as well as thermal loading is presented. The element includes the effect of shear deformation and involves five degree of freedom (three deflections and two rotation functions) per node. Numerical convergence of linear and quadratic elements is shown, and results are presented for single-layer and two-layer cylindrically curved cross-ply panels subjected to sinusoidal and uniform loadings: thermal, mechanical, and combined loadings are considered.

To check the finite-element results, a closed-form solution is developed herein for cross-ply cylindrically curved panels subjected to sinusoidal mechanical and/or thermal loadings. The exact solution can be obtained only under special conditions of geometry, edge conditions, and loadings. However, the finite-element formulation presented here does not have any limitations except for those implied in the formulation of the governing equations. The finite-element solutions are found to be in close agreement with the closed-form solutions for 2 by 2 mesh of quadratic elements in the quarter shell.

Thus, the finite element developed here is computationally simply compared to other cylindrical shell elements used previously in the thermal stress analysis of cylindrical shells.

Extension of the present element to non-linear thermal stress analysis and to thermal buckling analysis is recommended. In those cases, the present element should result in substantial savings.

ACKNOWLEDGMENTS

The authors are grateful to the Office of Naval Research, Structural Mechanics Program for financial support through Contract N00014-78-C-0647 and the University's Merrick Computing Center for providing computing time.

REFERENCES

1. S.K. Clark, The Plane Elastic Characteristics of Cord-Rubber Laminates, *Textile Research J.*, vol. 33, pp. 295-313, 1963.
2. H.P. Patel, J.L. Turner, and J.D. Walter, Radial Tire Cord-Rubber Composites, *Rubber Chem. Tech.*, vol. 49, pp. 1095-1110, 1976.
3. S.A. Ambartsumyan, The Basic Equations and Relations of the Different-Modulus Theory of Elasticity of an Anisotropic Body, *Mechanics of Solids*, vol. 4, no. 3, pp. 48-56, 1969.
4. C.W. Bert, Models for Fibrous Composites with Different Properties in Tension and Compression, *J. Eng. Matls. Tech., Trans. ASME*, vol. 99H, pp. 344-349, 1977.
5. C.W. Bert, Recent Advances in Mathematical Modeling of the Mechanical Behavior of Bimodulus, Fiber-Reinforced Composite Materials, *Proc., 15th Ann. Meeting, Soc. of Eng. Sci.*, Gainesville, FL, pp. 101-106, 1978.
6. S.A. Ambartsumyan, The Equations of Temperature Stresses of Different-Modulus Materials, *Mechanics of Solids*, vol. 3, no. 5, pp. 58-69, 1968.
7. S.A. Ambartsumyan, Equations of the Theory of Thermal Stresses in Double Modulus Materials, *Thermoelasticity* (Proc., IUTAM Sympos., E. Kilbride, Scotland, 1968), B.A. Boley, ed., Springer-Verlag, Wien, pp. 17-32, 1970.
8. N. Kamiya, Thermal Stress in a Bimodulus Thin Plate, *Bulletin de l'Academie Polonaise des Sciences, Serie des sciences techniques*, vol. 24, pp. 365-372, 1976.
9. N. Kamiya, Energy Formulae of Bimodulus Material in Thermal Field, *Fibre Sci. Tech.*, vol. 11, pp. 229-235, 1978.
10. N. Kamiya, Non-Stationary Thermal Stress in a Bimodulus Sphere, *Mech. Res. Comm.*, vol. 4, pp. 51-56, 1977.
11. N. Kamiya, Thermal Stress in a Bimodulus Thick Cylinder, *Nuclear Eng. Design*, vol. 40, pp. 383-391, 1977.
12. N. Kamiya, Thermoelasticity Considering Temperature-Dependent Material Properties, *Mechanics of Bimodulus Materials*, C.W. Bert, ed., ASME, NY, AMD-Vol. 33, pp. 29-37, 1979.
13. C.W. Bert, Micromechanics of the Different Elastic Behavior of Filamentary Composites in Tension and Compression, *Mechanics of Bimodulus Materials*, C.W. Bert, ed., ASME, NY, AMD-Vol. 33, pp. 17-28, 1979.
14. J.N. Reddy, C.W. Bert, Y.S. Hsu, and V.S. Reddy, Thermal Bending of Thick Rectangular Plates of Bimodulus Composite Materials, Report OU-AMNE-80-9, University of Oklahoma, Norman, OK, June 1980.

15. Y. Stavsky and I. Smolash, Thermoelasticity of Heterogeneous Orthotropic Cylindrical Shells, *Int. J. Solids Structures*, vol. 6, pp. 1211-1231, 1970.
16. Y.C. Pao, On Higher-Order Theory for Thermoelastic Analysis of Heterogeneous Orthotropic Cylindrical Shells, *Developments in Theoretical and Applied Mechanics*, vol. 6 (Proc., 6th SECTAM, Univ. of S. Fla., Tampa, 1972), pp. 787-806, 1972.
17. J. Padovan and J. Lestingi, Thermoelasticity of Anisotropic Cylindrical Shells, *J. Thermal Stresses*, vol. 3, pp. 261-276, 1980.
18. C.W. Bert and V.S. Reddy, Cylindrical Shells of Bimodulus Composite Material, Report OU-AMNE-80-3, School of Aerospace, Mechanical and Nuclear Engineering, University of Oklahoma, Norman, OK, Feb. 1980.
19. S.B. Dong and F.K.W. Tso, On a Laminated Orthotropic Shell Theory Including Transverse Shear Deformation, *Journal of Applied Mechanics*, vol. 39, pp. 1091-1096, 1972.
20. A.E.H. Love, On the Small Free Vibrations and Deformations of the Elastic Shells, *Phil. Trans. Roy. Soc. (London)*, ser. A, vol. 17, pp. 491-546, 1888. See also A.E.H. Love, *A Treatise on the Mathematical Theory of Elasticity*, 4th ed., Dover, NY, chap. 24, 1944.
21. E. Reissner, A New Derivation of the Equations for the Deformation of Elastic Shells, *Amer. J. Math.*, vol. 63, pp. 177-184, 1941.
22. H. Kraus, *Thin Elastic Shells*, Wiley, NY, 1967.
23. J.L. Sanders Jr., An Improved First Approximation Theory for Thin Shells, NASA TR R-24, June 1959. See also [21], pp. 59-65.
24. T.T. Loo, An Extension of Donnell's Equation for a Circular Cylindrical Shell, *J. Aeronaut. Sci.*, vol. 24, pp. 390-391, 1957.
25. L.S.D. Morley, An Improvement of Donnell's Approximation of Thin-Walled Circular Cylinders, *Quart. J. Mech. Appl. Math.*, vol. 8, pp. 169-176, 1959.
26. L.H. Donnell, Stability of Thin Walled Tubes in Torsion, NACA Rept. 479, 1933.
27. O.C. Zienkiewicz, R.L. Taylor, and J.M. Too, Reduced Integration Technique in General Analysis of Plates and Shells, *Int. J. Num. Meth. Eng.*, vol. 3, pp. 575-586, 1971.
28. J.N. Reddy, A Comparison of Closed-Form and Finite-Element Solutions of Thick, Laminated, Anisotropic Rectangular Plates, Report OU-AMNE-79-19, University of Oklahoma, Norman, OK, Dec. 1979.

29. B.A. Boley and J.H. Weiner, *Theory of Thermal Stresses*, pp. 389-391, Wiley, New York, 1960.
30. C.W. Bert, J.N. Reddy, V.S. Reddy, and W.C. Chao, Analysis of Thick Rectangular Plates Laminated of Bimodulus Composite Materials, *Proc., AIAA/ASME/ASCE/AHS 21st Structures, Structural Dynamics and Materials Conference*, Seattle, WA, May 1980, part 1, pp. 179-186.

APPENDIX A

DERIVATION OF EXPRESSIONS FOR THERMAL FORCES AND MOMENTS

Case I

For Case I, $z_{nx} > 0$ and $z_{ny} < 0$ with z_{nx} governing layer 1 (0°) and z_{ny} layer 2 (90°).

$$N_x^T = \int_{-h/2}^{z_{ny}} (Q_{1122} \alpha_{122} + Q_{1222} \alpha_{222}) T dz + \int_{z_{ny}}^0 (Q_{1112} \alpha_{112} + Q_{1212} \alpha_{212}) T dz \\ + \int_0^{z_{nx}} (Q_{1121} \alpha_{121} + Q_{1221} \alpha_{221}) T dz + \int_{z_{nx}}^{h/2} (Q_{1111} \alpha_{111} + Q_{1211} \alpha_{211}) T dz \quad (A-1)$$

Let

$$(Q_{1122} \alpha_{122} + Q_{1222} \alpha_{222}) = \beta_{122} \quad , \quad (Q_{1112} \alpha_{112} + Q_{1212} \alpha_{212}) = \beta_{112} \\ (Q_{1121} \alpha_{121} + Q_{1221} \alpha_{221}) = \beta_{121} \quad , \quad (Q_{1111} \alpha_{111} + Q_{1211} \alpha_{211}) = \beta_{111} \quad , \text{ etc.} \quad (A-2)$$

Then,

$$N_x^T = [\beta_{122} T_0(z_{ny} + h/2) + \beta_{112} T_0(0 - z_{ny}) + \beta_{121} T_0(z_{nx} - 0) \\ + \beta_{111} T_0(h/2 - z_{nx}) + \beta_{122}(T_1/2h)(z_{ny}^2 - h^2/4) \\ + \beta_{112}(T_1/2h)(0 - z_{ny}^2) + \beta_{121}(T_1/2h)(z_{nx}^2 - 0) \\ + \beta_{111}(T_1/2h)(h^2/4 - z_{nx}^2)] \sin \alpha x \sin \beta y \\ N_x^T = [(\beta_{122} + \beta_{111})(T_0 h/2) + (\beta_{121} - \beta_{111}) T_0 z_{nx} + (\beta_{122} - \beta_{112}) T_0 z_{ny} \\ + (\beta_{111} - \beta_{122})(T_1 h/8) + (\beta_{121} - \beta_{111})(T_1 z_{nx}^2/2h) \\ + (\beta_{122} - \beta_{112})(T_1 z_{ny}^2/2h)] \sin \alpha x \sin \beta y \quad (A-3)$$

Similarly,

$$\begin{aligned}
N_y^T = & [(\beta_{222} + \beta_{211})(T_0 h/2) + (\beta_{221} - \beta_{211}) T_0 z_{nx} + (\beta_{222} - \beta_{212}) T_0 z_{ny} \\
& + (\beta_{211} - \beta_{222})(T_1 h/8) + (\beta_{221} - \beta_{211})(T_1 z_{nx}^2/2h) + (\beta_{222} - \beta_{212}) \\
& (T_1 z_{ny}^2/2h)] \sin \alpha x \sin \beta y
\end{aligned} \tag{A-4}$$

Now,

$$\begin{aligned}
M_x^T = & \int_{-h/2}^{h/2} \beta_{122} T_z dz + \int_{z_{ny}}^0 \beta_{112} T_z dz + \int_0^{z_{nx}} \beta_{121} T_z dz + \int_{z_{nx}}^{h/2} \beta_{111} T_z dz \\
& [(\beta_{111} - \beta_{122})(T_0 h^2/8) + (\beta_{121} - \beta_{111})(T_0 z_{nx}^2/2) + (\beta_{122} - \beta_{112})(T_0 z_{ny}^2/2) \\
& + (\beta_{122} + \beta_{111})(T_1 h^2/24) + (\beta_{121} - \beta_{111})(T_1 z_{nx}^3/3h) \\
& + (\beta_{122} - \beta_{112})(T_1 z_{ny}^3/3h)] \sin \alpha x \sin \beta y
\end{aligned} \tag{A-5}$$

Similarly,

$$\begin{aligned}
M_y^T = & [(\beta_{211} - \beta_{222})(T_0 h^2/8) + (\beta_{221} - \beta_{211})(T_0 z_{nx}^2/2) + (\beta_{222} - \beta_{212})(T_0 z_{ny}^2/2) \\
& + (\beta_{222} + \beta_{211})(T_1 h^2/24) + (\beta_{221} - \beta_{212})(T_1 z_{nx}^3/3h) \\
& + (\beta_{222} - \beta_{212})(T_1 z_{ny}^3/3h)] \sin \alpha x \cos \beta y
\end{aligned} \tag{A-6}$$

Using the above equations in conjunction with equations (12) and (18), we obtain the following:

$$\begin{aligned}
R_{x,x}^T = & \alpha [(\beta_{122} + \beta_{111})(T_0 h/2) + (\beta_{121} - \beta_{111}) T_0 z_{nx} + (\beta_{122} - \beta_{112}) T_0 z_{ny} \\
& + (\beta_{111} - \beta_{122})(T_1 h/8) + (\beta_{121} - \beta_{111})(T_1 z_{nx}^2/2h) \\
& + (\beta_{122} - \beta_{112})(T_1 z_{ny}^2/2h)]
\end{aligned} \tag{A-7}$$

$$\begin{aligned} R_{t,y}^T = & \beta[(\beta_{222} + \beta_{211})(T_0 h/2) + (\beta_{221} - \beta_{211})T_0 z_{nx} + (\beta_{222} - \beta_{212})T_0 z_{ny} \\ & + (\beta_{211} - \beta_{222})(T_1 h/8) + (\beta_{221} - \beta_{211})(T_1 z_{nx}^2/2h) \\ & + (\beta_{222} - \beta_{212})(T_1 z_{ny}^2/2h)] \end{aligned} \quad (A-8)$$

$$\begin{aligned} R_{x,x}^T = & \alpha[(\beta_{111} - \beta_{122})(T_0 h^2/8) + (\beta_{121} - \beta_{111})(T_0 z_{nx}^2/2) + (\beta_{122} - \beta_{112}) \\ & (T_0 z_{ny}^2/2) + (\beta_{122} + \beta_{111})(T_1 h^2/24) + (\beta_{121} - \beta_{111})(T_1 z_{nx}^3/3h) \\ & + (\beta_{122} - \beta_{112})(T_1 z_{ny}^3/3h)] \end{aligned} \quad (A-9)$$

$$\begin{aligned} R_{y,y}^T = & \beta[(\beta_{211} - \beta_{222})(T_0 h^2/8) + (\beta_{221} - \beta_{211})(T_0 z_{nx}^2/2) + (\beta_{222} - \beta_{212})(T_0 z_{ny}^2/2) \\ & + (\beta_{222} + \beta_{211})(T_1 h^2/24) + (\beta_{221} - \beta_{211})(T_1 z_{nx}^3/3h) + (\beta_{222} - \beta_{212})(T_1 z_{ny}^3/3h)] \end{aligned} \quad (A-10)$$

In a similar way, one can obtain the expressions for the above-mentioned quantities for the remaining seven cases as follows:

Case II ($z_{nx} > 0, z_{ny} > 0$)

$$\begin{aligned} R_{x,x}^T = & \alpha[(\beta_{122} + \beta_{111})(T_0 h/2) + (\beta_{121} - \beta_{111})(T_0 z_{nx}) \\ & + (\beta_{111} - \beta_{122})(T_1 h/8) + (\beta_{121} - \beta_{111})(T_1 z_{nx}^2/2h)] \\ R_{y,y}^T = & \beta[(\beta_{222} + \beta_{211})(T_0 h/2) + (\beta_{221} - \beta_{211})(T_0 z_{nx}) \\ & + (\beta_{211} - \beta_{222})(T_1 h/8) + (\beta_{221} - \beta_{211})(T_1 z_{nx}^2/2h)] \end{aligned} \quad (A-11)$$

$$\begin{aligned} R_{x,x}^T = & \alpha[(\beta_{111} - \beta_{122})(T_0 h^2/8) + (\beta_{121} - \beta_{111})(T_0 z_{nx}^2/2) \\ & + (\beta_{122} + \beta_{111})(T_1 h^2/24) + (\beta_{121} - \beta_{111})(T_1 z_{nx}^3/3h)] \\ R_{y,y}^T = & \beta[(\beta_{211} - \beta_{222})(T_0 h^2/8) + (\beta_{221} - \beta_{211})(T_0 z_{nx}^2/2) \\ & + (\beta_{222} - \beta_{211})(T_1 h^2/24) + (\beta_{221} - \beta_{211})(T_1 z_{nx}^3/3h)] \end{aligned}$$

Case III ($z_{nx} < 0, z_{ny} > 0$)

$$\begin{aligned} \bar{N}_{x,x}^T = & \alpha[(\beta_{122} + \beta_{111})(T_0 h/2) + (\beta_{121} - \beta_{111})(T_0 z_{ny}) \\ & + (\beta_{122} - \beta_{112})(T_0 z_{nx}) + (\beta_{111} - \beta_{122})(T_1 h/8) \\ & + (\beta_{121} - \beta_{111})(T_1 z_{ny}^2/2h) + (\beta_{122} - \beta_{112})(T_1 z_{nx}^2/2h)] \end{aligned}$$

$$\begin{aligned} \bar{N}_{y,y}^T = & \beta[(\beta_{222} + \beta_{211})(T_0 h/2) + (\beta_{221} - \beta_{211})(T_0 z_{ny}) \\ & + (\beta_{222} - \beta_{212})(T_0 z_{nx}) + (\beta_{211} - \beta_{222})(T_1 h/8) \\ & + (\beta_{221} - \beta_{211})(T_1 z_{ny}^2/2h) + (\beta_{222} - \beta_{212})(T_1 z_{nx}^2/2h)] \end{aligned}$$

(A-12)

$$\begin{aligned} \bar{M}_{x,x}^T = & \alpha[(\beta_{111} - \beta_{122})(T_0 h^2/8) + (\beta_{121} - \beta_{111})(T_0 z_{ny}^2/2) \\ & + (\beta_{122} - \beta_{112})(T_0 z_{nx}^2/2) + (\beta_{122} + \beta_{111})(T_1 h^2/24) \\ & + (\beta_{121} - \beta_{111})(T_1 z_{ny}^3/3h) + (\beta_{122} - \beta_{112})(T_1 z_{nx}^3/3h)] \end{aligned}$$

$$\begin{aligned} \bar{M}_{y,y}^T = & [\beta_{211} - \beta_{222})(T_0 h^2/8) + (\beta_{221} - \beta_{211})(T_0 z_{ny}^2/2) \\ & + (\beta_{222} - \beta_{212})(T_0 z_{nx}^2/2) + (\beta_{222} + \beta_{211})(T_1 h^2/24) \\ & + (\beta_{221} - \beta_{211})(T_1 z_{ny}^3/3h) + (\beta_{222} - \beta_{212})(T_1 z_{nx}^3/3h)] \end{aligned}$$

Case IV ($z_{nx} < 0, z_{ny} < 0$)

$$\begin{aligned} \bar{N}_{x,x}^T = & \alpha[(\beta_{122} + \beta_{111})(T_0 h/2) + (\beta_{122} - \beta_{121})(T_0 z_{ny}) \\ & + (\beta_{111} - \beta_{122})(T_1 h/8) + (\beta_{122} - \beta_{121})(T_1 z_{ny}^2/2h)] \end{aligned}$$

$$\begin{aligned} \bar{N}_{y,y}^T = & \beta[(\beta_{222} + \beta_{211})(T_0 h/2) + (\beta_{222} - \beta_{221})(T_0 z_{ny}) \\ & + (\beta_{211} - \beta_{222})(T_1 h/8) + (\beta_{222} - \beta_{221})(T_1 z_{ny}^2/2h)] \end{aligned}$$

(A-13)

$$R_{x,x}^T = \alpha[(\beta_{111} - \beta_{122})(T_0 h^2/8) + (\beta_{122} - \beta_{121})(T_0 z_{ny}^2/2) + (\beta_{122} + \beta_{111})(T_1 h^2/24) + (\beta_{122} - \beta_{121})(T_1 z_{ny}^3/3h)] \quad (A-13 \text{ cont.})$$

$$R_{y,y}^T = \beta[(\beta_{211} - \beta_{222})(T_0 h^2/8) + (\beta_{222} - \beta_{221})(T_0 z_{ny}^2/2) + (\beta_{222} + \beta_{211})(T_1 h^2/24) + (\beta_{222} - \beta_{221})(T_1 z_{ny}^3/3h)]$$

For neutral surface going out of plane,

Case V ($z_{nx} > 0.5$, $z_{ny} < -0.5$)

$$\begin{aligned} R_{x,x}^T &= \alpha[(\beta_{121} + \beta_{112})(T_0/2) + (\beta_{121} - \beta_{112})(T_1/8)] \\ R_{y,y}^T &= \beta[(\beta_{221} + \beta_{212})(T_0/2) + (\beta_{221} - \beta_{212})(T_1/8)] \\ R_{x,x}^T &= \alpha[(\beta_{121} - \beta_{112})(T_0/8) + (\beta_{121} + \beta_{112})(T_1/24)] \\ R_{y,y}^T &= \beta[(\beta_{221} - \beta_{212})(T_0/8) + (\beta_{221} + \beta_{212})(T_1/24)] \end{aligned} \quad (A-14)$$

Case VI ($z_{nx} < -0.5$, $z_{ny} > 0.5$)

$$\begin{aligned} R_{x,x}^T &= \alpha[(\beta_{121} + \beta_{112})(T_0/2) + (\beta_{121} - \beta_{112})(T_1/8)] \\ R_{y,y}^T &= \beta[(\beta_{221} + \beta_{212})(T_0/2) + (\beta_{221} - \beta_{212})(T_1/8)] \\ R_{x,x}^T &= \alpha[(\beta_{121} - \beta_{112})(T_0/8) + (\beta_{121} + \beta_{112})(T_1/24)] \\ R_{y,y}^T &= \beta[(\beta_{221} - \beta_{212})(T_0/8) + (\beta_{221} + \beta_{212})(T_1/24)] \end{aligned} \quad (A-15)$$

Case VII ($z_{nx} > 0.5$, $z_{ny} > 0.5$)

$$\begin{aligned} R_{x,x}^T &= \alpha[(\beta_{111} + \beta_{112})(T_0/2) + (\beta_{111} - \beta_{112})(T_1/8)] \\ R_{y,y}^T &= \beta[(\beta_{211} + \beta_{212})(T_0/2) + (\beta_{211} - \beta_{212})(T_1/8)] \\ R_{x,x}^T &= \alpha[(\beta_{111} - \beta_{112})(T_0/8) + (\beta_{111} + \beta_{112})(T_1/24)] \\ R_{y,y}^T &= \beta[(\beta_{211} - \beta_{212})(T_0/8) + (\beta_{211} + \beta_{212})(T_1/24)] \end{aligned} \quad (A-16)$$

Case VIII ($z_{nx} < -0.5$, $z_{ny} < -0.5$)

$$R_{x,x}^T = \alpha[(\beta_{121} + \beta_{122})(T_0/2) + (\beta_{121} - \beta_{122})(T_1/8)]$$

$$R_{y,y}^T = \beta[(\beta_{221} + \beta_{222})(T_0/2) + (\beta_{221} - \beta_{222})(T_1/8)]$$

(A-17)

$$R_{x,x}^T = \alpha[(\beta_{121} - \beta_{122})(T_0/8) + (\beta_{121} + \beta_{122})(T_1/24)]$$

$$R_{y,y}^T = \beta[(\beta_{221} - \beta_{222})(T_0/8) + (\beta_{221} + \beta_{222})(T_1/24)]$$

For a single layer, change β_{112} to β_{111} , β_{122} to β_{121} , β_{212} to β_{211} and

β_{222} to β_{221} .

APPENDIX B
LISTING OF COEFFICIENTS OF STIFFNESS MATRIX
AND FORCE VECTOR FOR FINITE-ELEMENT FORMULATION

The elements of the stiffness-matrix appearing in Equation (25) are:

$$\begin{aligned}
 K_{ij}^{11} &= A_{11}G_{ij}^x + (A_{66} - \bar{c}_2B_{66} + \frac{1}{4}\bar{c}_2^2D_{66})G_{ij}^y \\
 K_{ij}^{12} &= A_{12}G_{ij}^{xy} + (A_{66} - \frac{1}{4}\bar{c}_2^2D_{66})G_{ji}^{xy} \\
 K_{ij}^{13} &= (A_{12}/R)M_{ij}^{xo} \quad ; \quad K_{ij}^{14} = B_{11}H_{ij}^x + (B_{66} - \frac{1}{2}\bar{c}_2D_{66})H_{ij}^y \\
 K_{ij}^{15} &= B_{12}H_{ij}^{xy} + (B_{66} - \frac{1}{2}\bar{c}_2D_{66})H_{ji}^{xy} \\
 K_{ij}^{22} &= A_{22}G_{ij}^y + (A_{66} + \bar{c}_2B_{66} + \frac{1}{4}\bar{c}_2^2D_{66})G_{ij}^x + \bar{c}_1^2S_{44}G_{ij}^o \\
 K_{ij}^{23} &= (A_{22}/R)M_{ji}^{yo} \quad ; \quad K_{ij}^{24} = (B_{66} + \frac{1}{2}\bar{c}_2D_{66})H_{ij}^{xy} + B_{12}H_{ji}^{xy} \\
 K_{25} &= (B_{66} + \frac{1}{2}\bar{c}_2D_{66})H_{ij}^x + B_{22}H_{ij}^y - \bar{c}_1S_{44}H_{ij}^o \\
 K_{33} &= S_{55}S_{ij}^x + S_{44}S_{ij}^y + (A_{22}/R^2)S_{ij}^o \\
 K_{34} &= S_{55}R_{ij}^{xo} + (B_{12}/R)R_{ji}^{xo} \quad ; \quad K_{35} = S_{44}R_{ij}^{yo} + (B_{22}/R)R_{ji}^{yo} \\
 K_{44} &= D_{11}T_{ij}^x + D_{66}T_{ij}^x + D_{66}T_{ij}^y + S_{55}T_{ij}^o \quad ; \quad K_{45} = D_{12}T_{ij}^{xy} + D_{66}T_{ji}^{xy} \\
 K_{55} &= D_{66}T_{ij}^x + D_{22}T_{ij}^y + S_{44}T_{ij}^o
 \end{aligned} \tag{B-1}$$

The generalized-force elements appearing in Equation (25) are:

$$\begin{aligned}
 F_i^1 &= \int_{R_e} (N_{1,x}^T + N_{6,y}^T - \frac{1}{2}\bar{c}_2M_{6,y}^T)\phi_i^1 dx dy \\
 F_i^2 &= \int_{R_e} (N_{2,y}^T + N_{6,x}^T + \frac{1}{2}\bar{c}_2M_{6,x}^T)\phi_i^1 dx dy \\
 F_i^3 &= \int_{R_e} (P - N_2^T/R)\phi_i^2 dx dy \\
 F_i^4 &= \int_{R_e} (M_{1,x}^T + M_{6,y}^T)\phi_i^3 dx dy \quad ; \quad F_i^5 = \int_{R_e} (M_{2,y}^T + M_{6,x}^T)\phi_i^3 dx dy
 \end{aligned} \tag{B-2}$$

where

$$\begin{aligned}
 G_{ij}^{\xi n} &= \int_{R_e} \phi_{i,\xi}^1 \phi_{j,n}^1 dx dy & (i,j=1,2,\dots,r) \\
 H_{ij}^{\xi n} &= \int_{R_e} \phi_{i,\xi}^1 \phi_{j,n}^3 dx dy & (i=1,2,\dots,r ; j=1,2,\dots,t) \\
 M_{ij}^{\xi n} &= \int_{R_e} \phi_{i,\xi}^1 \phi_{j,n}^2 dx dy & (i=1,2,\dots,r ; j=1,2,\dots,s) \\
 S_{ij}^{\xi n} &= \int_{R_e} \phi_{i,\xi}^2 \phi_{j,n}^2 dx dy & (i,j=1,2,\dots,s) \\
 R_{ij}^{\xi n} &= \int_{R_e} \phi_{i,\xi}^2 \phi_{j,n}^3 dx dy & (i=1,2,\dots,s ; j=1,2,\dots,t) \\
 T_{ij}^{\xi n} &= \int_{R_e} \phi_{i,\xi}^3 \phi_{j,n}^3 dx dy & (i,j=1,2,\dots,s)
 \end{aligned}
 \tag{B-3}$$

($\xi, n=0, x, y$)

and $G_{ij}^{xx} = G_{ij}^x$, etc. In the special case in which $\phi_i^1 = \phi_i^2 = \phi_i^3$, all of the matrices in Equation (B-3) coincide.

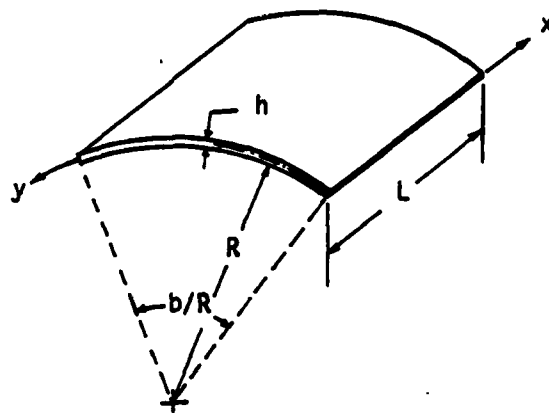


Figure 1. Shell geometry

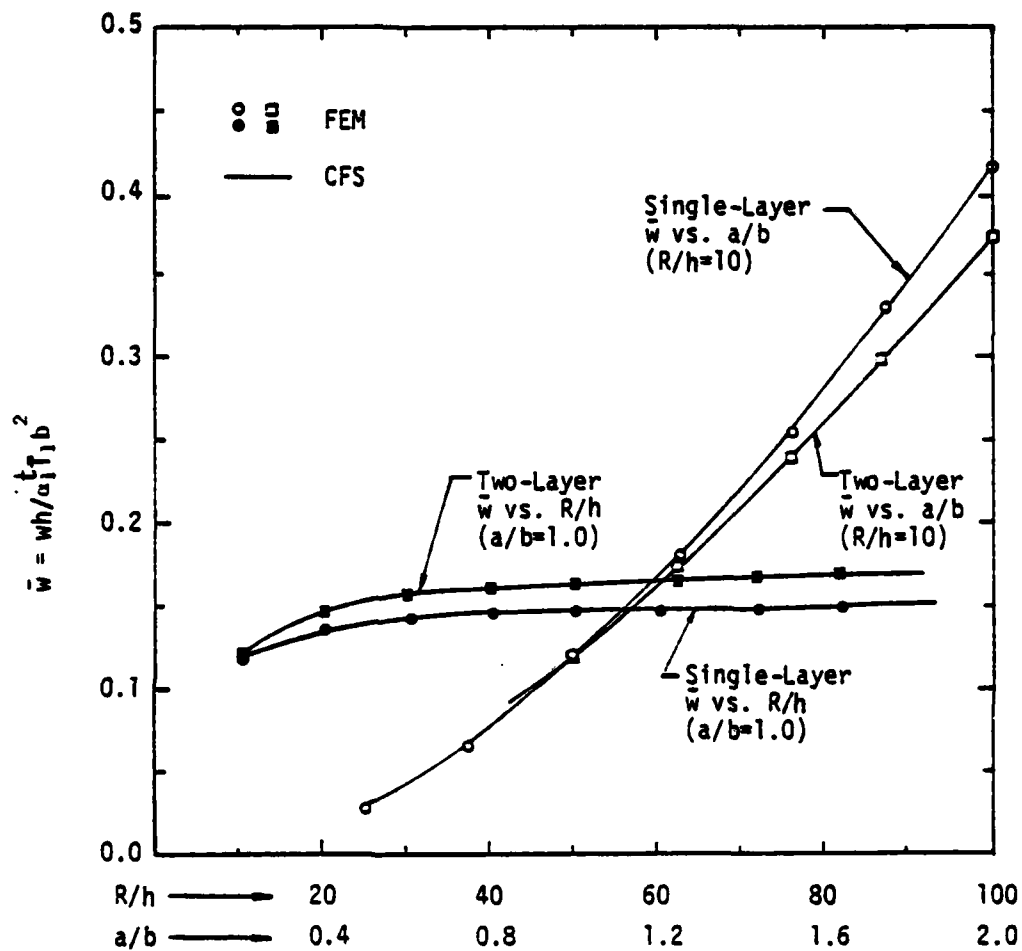


Figure 2. Transverse deflection vs. aspect ratio and radius-to-thickness ratio for single-layer and two-layer cross-ply cylindrical panels under sinusoidal thermal loading by Sanders theory (Material: aramid-rubber).

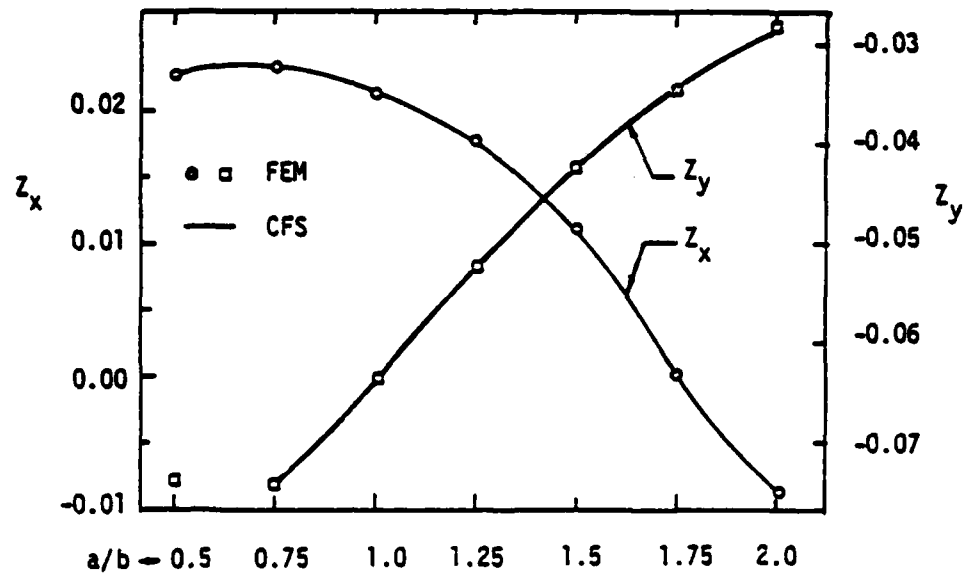


Figure 3. Neutral-surface location vs. aspect ratio for single-layer cylindrical shells under sinusoidal thermal loading by Sanders theory (Material: aramid-rubber, $R/h=10$)

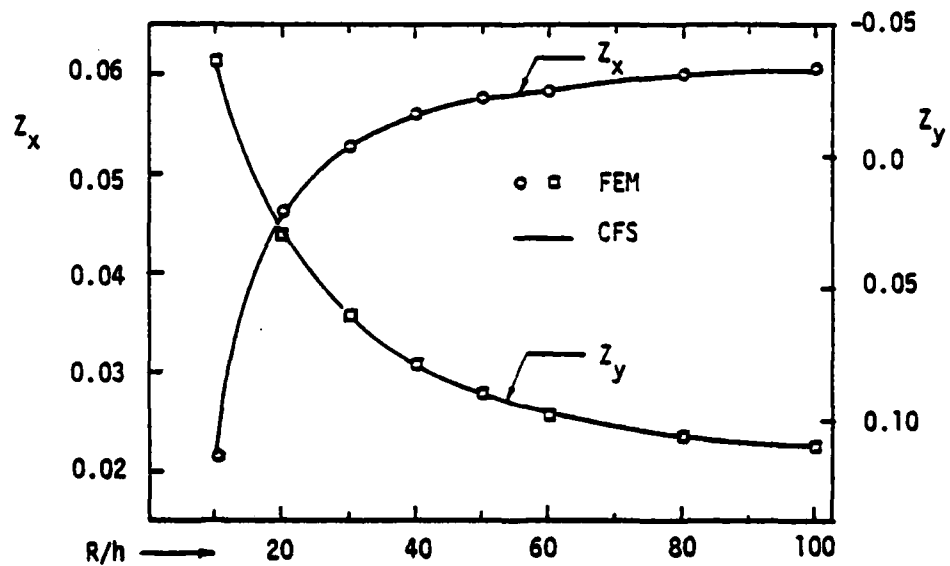


Figure 4. Neutral-surface location vs. radius-to-thickness ratio for single-layer cylindrical shell under sinusoidal thermal loading by Sanders theory (Material: aramid-rubber, $a/b=1.0$).

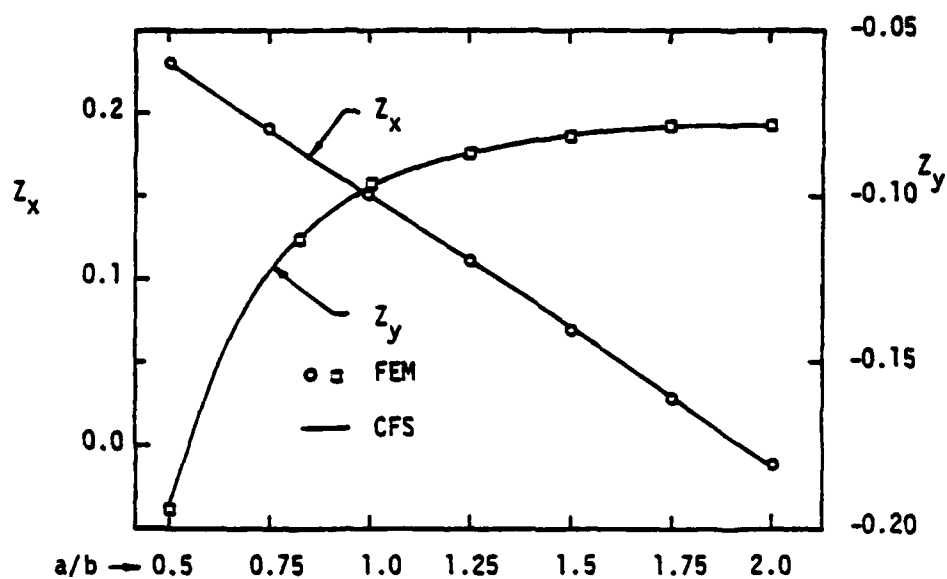


Figure 5. Neutral-surface location vs. aspect ratio for two-layer cross-ply($0^\circ/90^\circ$) cylindrical shells under sinusoidal thermal loading by Sanders theory (Material: polyester-rubber, $R/h=10$).

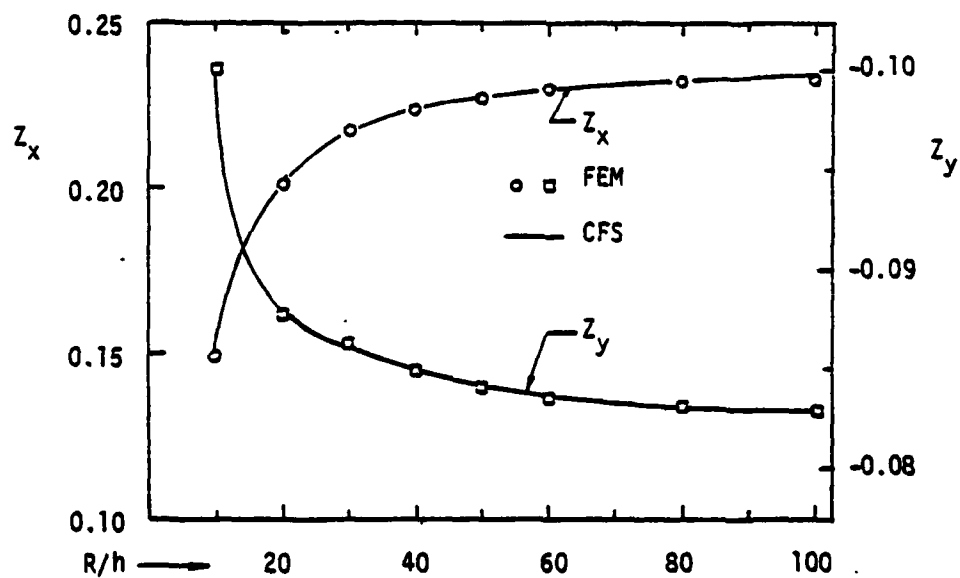


Figure 6. Neutral-surface location vs. radius-to-thickness ratio for two-layer($0^\circ/90^\circ$) cylindrical shells under sinusoidal thermal loading by Sanders theory (Material: polyester-rubber, $a/b=1.0$).

Table 1. List of Shell-Theory Tracers and Their Values

Theory (Thin-Shell Theory Generalized to Shear-Flexible Theory)	C_1	C_2
Sanders'	1	1
Love's first approximation and Loo's	1	0
Morley's and Donnell's	0	0

Table 2. Elastic Properties for Two Tire-Cord/Rubber, Unidirectional, Bimodulus Composite Materials^a

Property and Units	Aramid-Rubber		Polyester-Rubber	
	k=1	k=2	k=1	k=2
Longitudinal Young's modulus, GPa	3.58	0.0120	0.617	0.0369
Transverse Young's modulus, GPa	0.00909	0.0120	0.00800	0.0106
Major Poisson's ratio, dimensionless ^b	0.416	0.205	0.475	0.185
Longitudinal-transverse shear modulus, GPa ^c	0.00370	0.00370	0.00262	0.00267
Transverse-thickness shear modulus, GPa	0.00290	0.00499	0.00233	0.00475

^aFiber-direction tension is denoted by k=1, and fiber-direction compression by k=2.

^bIt is assumed that the minor Poisson's ratio is given by the reciprocal relation.

^cIt is assumed that the longitudinal-thickness shear modulus is equal to this one.

Table 3. Effect of the radius-to-thickness ratio (R/h) on the locations of neutral surfaces and deflections for single- and two-layer, cross-ply, aramid-rubber cylindrical panels under sinusoidal loading by the Sanders theory ($T_1 = T_0 = 0$, $a/b = 1$, $b/h = 10$, material I).

R/h	Layers	Source	\bar{w}	Z_x	Z_y
$R/h \rightarrow \infty$ (plate)	1	CF	0.02094	0.44205	-0.16185
		FEM	0.02093	0.44205	-0.1616
	2	CF	0.01982	0.4384	-0.03418
		FEM	0.01981	0.4384	-0.03416
100	1	CF	0.020246	0.4408	-0.1840
		FEM	0.020234	0.4408	-0.1838
	2	CF	0.01892	0.43666	-0.036686
		FEM	0.01891	0.43661	-0.03666
50	1	CF	0.01943	0.4396	-0.2065
		FEM	0.01943	0.4396	-0.2063
	2	CF	0.01793	0.4350	-0.03909
		FEM	0.01793	0.4350	-0.03905
40	1	CF	0.01900	0.4390	-0.2179
		FEM	0.01899	0.4390	-0.2177
	2	CF	0.01742	0.4341	-0.04027
		FEM	0.01741	0.4341	-0.04022
20	1	CF	0.01663	0.4361	-0.2769
		FEM	0.01663	0.4361	-0.2767
	2	CF	0.01478	0.4300	-0.04600
		FEM	0.01478	0.4300	-0.04593
10	1	CF	0.01206	0.4305	-0.4127
		FEM	0.01206	0.4305	-0.4127
	2	CF	0.01019	0.4221	-0.05766
		FEM	0.01019	0.4221	-0.05752
5	1	CF	0.006223	0.4200	-0.8655
		FEM	0.006223	0.4200	-0.8655
	2	CF	0.004975	0.4070	-0.09156
		FEM	0.004972	0.4070	-0.09057

$$* \bar{w} = \frac{W E h^3}{P_0 a^4}, \quad Z_x = z_{nx}/h, \quad Z_y = z_{ny}/h$$

Table 4. Neutral-surface positions and dimensionless deflections for cylindrical panels of single-layer (0°) aramid-rubber and polyester-rubber under sinusoidal thermal loading, as determined by two different methods. (R/h = 10.0, $T_1 = 1.0$, $T_0 = 0.0$, $P_0 = 0$).*

Aspect Ratio a/b	\bar{w}		Z_x		Z_y	
	C.F.	F.E.	C.F.	F.E.	C.F.	F.E.
Aramid-Rubber						
0.5	0.03016	0.03021	0.02250	0.02247	-0.07431	-0.07308
0.75	0.06767	0.06772	0.02295	0.02295	-0.07458	-0.07400
1.0	0.1190	0.1190	0.021565	0.02158	-0.06347	-0.06332
1.25	0.1821	0.1821	0.01772	0.01768	-0.05191	-0.05157
1.5	0.2545	0.2546	0.01124	0.01121	-0.04228	-0.04204
1.75	0.3331	0.3330	0.002360	0.02314	-0.03473	-0.03454
2.0	0.41505	0.4149	-0.0085575	0.08476	-0.02892	-0.02876
Polyester-Rubber						
0.5	0.04083	0.04088	0.09004	0.08958	-0.2011	-0.1978
0.75	0.08952	0.08955	0.08481	0.08463	-0.1574	-0.1560
1.0	0.1527	0.1527	0.07445	0.07423	-0.1112	-0.1109
1.25	0.2263	0.2263	0.06020	0.06919	-0.07815	-0.07779
1.5	0.3060	0.3059	0.04302	0.04300	-0.05596	-0.05573
1.75	0.3881	0.3880	0.02370	0.02364	-0.04104	-0.04088
2.0	0.4695	0.4693	0.002851	0.002742	-0.03082	-0.03069

$$* \bar{w} = \frac{\bar{w}h}{\alpha_1 T_1 b^2}, \quad Z_x = z_{nx}/h, \quad Z_y = z_{ny}/h$$

Table 5. Neutral-surface positions and dimensionless deflections for cylindrical panel of two-layer (0°/90°) aramid-rubber and polyester-rubber under sinusoidal thermal loading. ($R/h = 10.0$, $T_1 = 1.0$, $T_0 = 0.0$, $P_0 = 0$).*

Aspect Ratio a/b	\bar{w}		Z_x		Z_y	
	C.F.	F.E.	C.F.	F.E.	C.F.	F.E.
Aramid-Rubber						
1.0	0.1212	0.1218	0.05189	0.05335	-0.05085	-0.05133
1.25	0.1783	0.1787	0.03656	0.03763	-0.04511	-0.04644
1.5	0.2408	0.2410	0.02050	0.02084	-0.04052	-0.04209
1.75	0.3064	0.3065	0.003910	0.004119	-0.03682	-0.03694
2.0	0.3726	0.3726	-0.01397	-0.001406	-0.03387	-0.03493
Polyester-Rubber						
1.0	0.1829	0.1849	0.1486	0.1510	-0.09623	-0.1006
1.25	0.23745	0.2399	0.1066	0.1100	-0.08727	-0.08823
1.5	0.2882	0.2905	0.06572	0.06857	-0.08188	-0.08287
1.75	0.33435	0.3363	0.02652	0.02813	-0.07857	-0.08074
2.0	0.37525	0.3769	0.01112	-0.01144	-0.07649	-0.07866

$$^* \bar{w} = \frac{\bar{w}h}{t_1 b^2}, \quad Z_x = z_{nx}/h, \quad Z_y = z_{ny}/h$$

PREVIOUS REPORTS ON THIS CONTRACT

<u>Project Rept. No.</u>	<u>OU-AMNE Rept. No.</u>	<u>Title of Report</u>	<u>Author(s)</u>
1	79-7	Mathematical Modeling and Micromechanics of Fiber-Reinforced Bimodulus Composite Material	C.W. Bert
2	79-8	Analyses of Plates Constructed of Fiber-Reinforced Bimodulus Materials	J.N. Reddy and C.W. Bert
3	79-9	Finite-Element Analyses of Laminated Composite-Material Plates	J.N. Reddy
4A	79-10A	Analyses of Laminated Bimodulus Composite-Material Plates	C.W. Bert
5	79-11	Recent Research in Composite and Sandwich Plate Dynamics	C.W. Bert
6	79-14	A Penalty-Plate Bending Element for the Analysis of Laminated Anisotropic Composite Plates	J.N. Reddy
7	79-18	Finite-Element Analysis of Laminated Bimodulus Composite-Material Plates	J.N. Reddy and W.C. Chao
8	79-19	A Comparison of Closed-Form and Finite-Element Solutions of Thick Laminated Anisotropic Rectangular Plates (With a Study of the Effect of Reduced Integration on the Accuracy)	J.N. Reddy
9	79-20	Effects of Shear Deformation and Anisotropy on the Thermal Bending of Layered Composite Plates	J.N. Reddy and Y.S. Hsu
10	80-1	Analyses of Cross-Ply Rectangular Plates of Bimodulus Composite Material	V.S. Reddy and C.W. Bert
11	80-2	Analysis of Thick Rectangular Plates Laminated of Bimodulus Composite Materials	C.W. Bert, J.N. Reddy, V.S. Reddy, and W.C. Chao
12	80-3	Cylindrical Shells of Bimodulus Composite Material	C.W. Bert and V.S. Reddy
13	80-6	Vibration of Composite Structures	C.W. Bert
14	80-7	Large Deflection and Large-Amplitude Free Vibrations of Laminated Composite-Material Plates	J.N. Reddy and W.C. Chao
15	80-8	Vibration of Thick Rectangular Plates of Bimodulus Composite Material	C.W. Bert, J.N. Reddy, W.C. Chao, and V.S. Reddy
16	80-9	Thermal Bending of Thick Rectangular Plates of Bimodulus Material	J.N. Reddy, C.W. Bert, Y.S. Hsu, and V.S. Reddy

UNCLASSIFIED

SECURITY CLASSIFICATION OF THIS PAGE (When Data Entered)

REPORT DOCUMENTATION PAGE		READ INSTRUCTIONS BEFORE COMPLETING FORM
1. REPORT NUMBER OU-AMNE-80-14	2. GOVT ACCESSION NO. AD-A089429	3. RECIPIENT'S CATALOG NUMBER
4. TITLE (and Subtitle) THERMOELASTICITY OF CIRCULAR CYLINDRICAL SHELLS LAMINATED OF BIMODULUS COMPOSITE MATERIALS		5. TYPE OF REPORT & PERIOD COVERED Technical Report No. 17
7. AUTHOR(s) Y.S. Hsu, J.N. Reddy, and C.W. Bert		6. PERFORMING ORG. REPORT NUMBER
9. PERFORMING ORGANIZATION NAME AND ADDRESS School of Aerospace, Mechanical and Nuclear Engineering University of Oklahoma, Norman, OK 73019		8. CONTRACT OR GRANT NUMBER(s) N00014-78-C-0647
11. CONTROLLING OFFICE NAME AND ADDRESS Department of the Navy, Office of Naval Research Structural Mechanics Program (Code 474) Arlington, Virginia 22217		10. PROGRAM ELEMENT, PROJECT, TASK AREA & WORK UNIT NUMBERS NR 064-609
14. MONITORING AGENCY NAME & ADDRESS (if different from Controlling Office)		12. REPORT DATE July 1980
		13. NUMBER OF PAGES 35
		15. SECURITY CLASS. (of this report) UNCLASSIFIED
		15a. DECLASSIFICATION/DOWNGRADING SCHEDULE
16. DISTRIBUTION STATEMENT (of this Report) This document has been approved for public release and sale; distribution unlimited.		
17. DISTRIBUTION STATEMENT (of the abstract entered in Block 20, if different from Report)		
18. SUPPLEMENTARY NOTES		
19. KEY WORDS (Continue on reverse side if necessary and identify by block number) Bimodulus materials, classical solutions, closed-form solutions, composite materials, fiber-reinforced materials, finite-element analysis, laminated shells, moderately thick shells, shell theory, thermal expansion, thermal stresses, thermoelasticity, transverse shear deformation.		
20. ABSTRACT (Continue on reverse side if necessary and identify by block number) Closed-form and finite-element solutions are presented for the thermoelastic behavior of laminated composite shells. The material of each layer is assumed to be thermoelastically orthotropic and bimodular, i.e., having different properties depending upon whether the fiber-direction normal strain is tensile or compressive. The formulations are based on the thermoelastic generalization of Dong and Tso's laminated shell theory, which includes thickness shear deformations. The finite element used here has five (over)		

DD FORM 1 JAN 73 1473

EDITION OF 1 NOV 65 IS OBSOLETE
S/N 0102-010-0001

UNCLASSIFIED

SECURITY CLASSIFICATION OF THIS PAGE (When Data Entered)

UNCLASSIFIED

SECURITY CLASSIFICATION OF THIS PAGE(When Data Entered)

20. Abstract - Cont'd

degrees of freedom per node (three displacements and two bending slopes). Numerical results are presented for deflections and the positions of the neutral surfaces associated with bending along both coordinate directions. The closed-form and finite-element results are found to be in good agreement.

UNCLASSIFIED

SECURITY CLASSIFICATION OF THIS PAGE(When Data Entered)

